The effect of climate change on the mobility and stability of coastal sand dunes in Ceará State (NE Brazil)

Haim Tsoar [a,*], Noam Levin [b], Naomi Porat [c], Luis P. Maia [d], Hans J. Herrmann [e], Sonia H. Tatumi [f], Vanda Claudino-Sales [g]

[a] Department of Geography and Environmental Development, Ben-Gurion University of the Negev, Beer Sheva 84105, Israel
[b] Department of Geography, Hebrew University of Jerusalem, Jerusalem 91905, Israel
[c] Geological Survey of Israel, Jerusalem 95301, Israel
[d] Instituto de Ciências do Mar — LABOMAR, Av. Abolicão, 3207, Meireles, Fortaleza, Ceará, Brazil
[e] The Swiss Federal Institute of Technology Zurich, Computational Physics, ETH-Hönggerberg, Institut für Baustoffe (IfB), HIF E 12, Schafmattstr. 6,8093 Zürich, Switzerland
[f] Laboratório de Vidros e Datação, Faculdade de Tecnologia de São Paulo, Centro Estadual de Educação Tecnológica, São Paulo, SP, Brazil
[g] Departamento de Geografia, Universidade Federal do Ceará, 60451-970 Fortaleza, Ceará, Brazil

ARTICLE INFO

ABSTRACT

The coast of Ceará State in NE Brazil is covered by vast fields of active and stabilized coastal sand dunes. Its tropical climate is characterized by two seasons, wet and dry, with wind intensity determined by the meridional shift of the Intertropical Convergence Zone. The wind power is negatively correlated with precipitation, and precipitation is negatively correlated with the difference between sea surface temperatures of the tropical Atlantic north and south of the equator. We present a model suggesting that during the Late Pleistocene wind power determined the mobility and stability of the dunes. Sand dunes accumulated during periods of high wind power (as it is today) and stabilized when wind power was low. Once the dunes were stabilized by vegetation they could not be activated even by increased wind power. Samples that were taken for luminescence dating from 25 stabilized dunes along the coasts of Ceará gave ages ranging from135 ka to <100 yr. We postulate that these luminescence ages fall at the beginning of wet periods in NE Brazil characterized by low wind power. These paleoclimatic wet periods correlate well with the cold periods of stades in Greenland ice-core records.

© 2008 University of Washington. All rights reserved.

Introduction

The coastal zone of Ceará State in NE Brazil, stretches for 572 km and consists of sandy beaches that feed vast coastal dunes in the hinterland. These dune fields form mostly on the coastline pointing SE to NW, and are nearly perpendicular to the easterly trade-winds (Fig. 1). Because of the unidirectional, powerful trade-winds, the Ceará coastal dunes are large, reaching heights of 13–25 m, and exhibit high rates of advance (Castro, 2005; Jimenez et al., 1999).

The coastal sand dunes of Ceará State are composed of active barchan and transverse dunes with fixed parabolic dunes in the hinterland (Claudino-Sales and Peulvast, 2002; Fig. 1). All stabilized dunes imply past activity followed by stabilization due to changes in climate. It is assumed that several cycles of beach-sand incursion took place, which were followed by stabilization. Previous studies have indicated that these incursions took place roughly during the Late Pleistocene and Early Holocene (Claudino-Sales and Peulvast 2002; Jimenez et al., 1999; De Oliveira et al., 1999).

This paper will present a model that explains the coexistence of active and stabilized sand dunes along the Ceará coast and explore the climatic conditions that brought about stabilization of the previously active dunes. We will also explain why so many active dunes are found today in the region, where the climate is humid and the average annual precipitation is above 1000 mm. Conditions that caused incursion and stabilization of the NE Brazil coastal sand dunes are depicted, based on climate fluctuations in the Tropical Atlantic during the Late Quaternary.

Models of mobility and stability of coastal sand dunes

The climatic conditions that determine vegetation cover on sand dunes are related to the fraction of time that wind speed is above the threshold velocity for sand transport (W) and the ratio between annual precipitation and potential evaporation (P/PE) (Ash and Wasson, 1983; Wasson, 1984). The sand-mobility or M-index of Lancaster (1988) is one of the best known, commonly used indices based on these parameters. It is defined as the quotient of W and P/PE. Lancaster (1988) calibrated his M-index in the dunefields of Southern Africa, where he found that $M < 50$ refers to fully stabilized dunes and $M > 200$ refers to fully active dunes. M values between these two
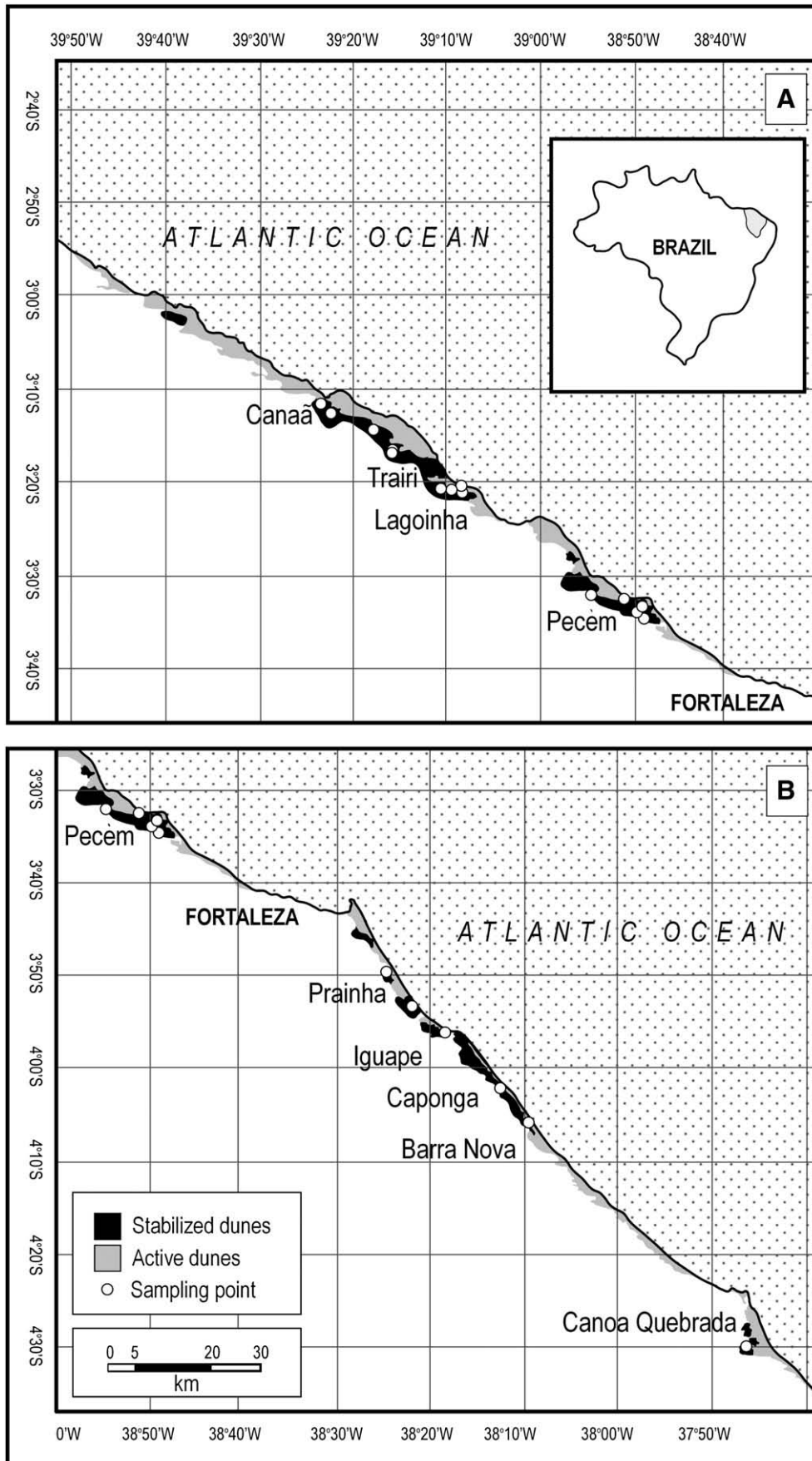

Figure 1. Map of coastal dunes (active and stabilized) along the coasts of Ceará State (shown on the small map of Brazil). (A) The western part of the coast. (B) The eastern part of the coast. White dots indicate the location of stabilized dunes from which sand samples were taken for luminescence dating and redness index determination.

Figure 2. Active transverse dune, bare of vegetation and stabilized dunes in the background, near Pecém, west of Fortaleza.

values indicate dunes undergoing gradual transition from full stability to full activity.

For Papicu beach, near Fortaleza, the average values of precipitation and potential evaporation, are: $P = 1519$ mm and $PE = 1804$ mm, with $P/PE = 0.84$, a ratio characteristic of humid climates (Middleton and Thomas, 1997). Because W for Fortaleza is 59%, its M-index equals 70. From Lancaster's M-index calibration, the Fortaleza dunes should be covered by vegetation with activity taking place only on their crests. However, the coastal dunes of Ceará are either fully stabilized with vegetation covering the whole dune along with the interdune area, or they are fully active with no vegetative cover (Fig. 2). The coexistence of active and fixed dunes in the same area cannot be explained by the assumptions underlying Lancaster's M-index.

A recent hysteresis model (Yizhaq et al., 2007) explains bistability of active and stabilized dunes under the same climate conditions (Fig. 3). In this model, the effect of wind power on vegetative cover is

taken into account. On the Ceará coast, as long as $P > 400$ mm, there is no restriction on vegetation growth. Even during Brazil's driest years of the last 160 yr, rainfall in Fortaleza was never lower than 400 mm.

Wind power — which varies with the cube of wind velocity — is one of the most important climatic factor determining the formation and activation of sand dunes (Tsoar 2005). The effect of wind power on sand dune movement is generally given in terms of a *drift potential* (*DP*) equation that is determined by a function based on the cube of wind velocity (Fryberger, 1979). This is given as

$$DP = \sum \frac{U^2(U-U_t)}{100} t \tag{1}$$

where U is the wind velocity (in knots) measured at a height of 10 m, U_t is the threshold wind velocity ($=12$ knots) and t is the percentage of time that wind velocity was above U_t. We divide by 100 to produce a
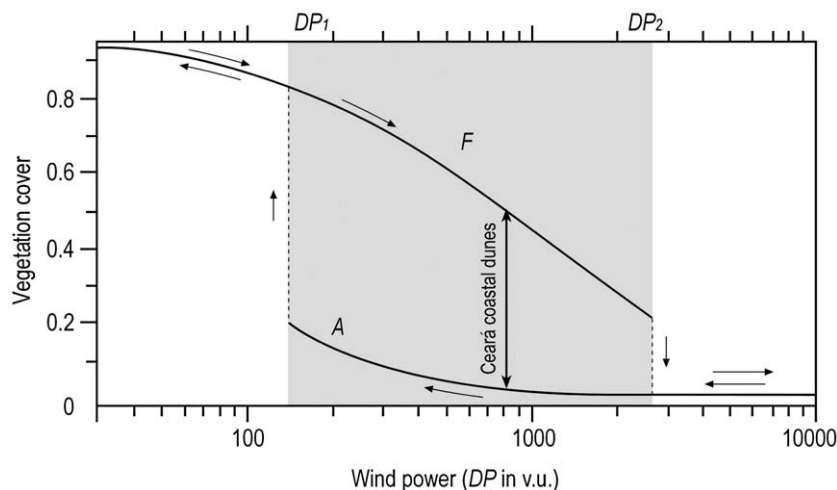

Figure 3. The hysteresis model that shows the dependence of vegetation cover on wind power. The solid lines indicate the two stable states: *F*, for the fixed-dune state and *A* for the active-dune state. The gray area indicates the zone of bistability, which is characteristic of the situation existing at the Ceará coast. When average wind power is reduced, active dunes will slow down and start to develop vegetation cover that eventually causes them to become fixed. When the climate changes and average wind power increases to high values, the fixed vegetated dune can become active. The dashed lines in the figure show the locations of the two one way transitions from activity to stability and vice versa, which fall at *DP*1 ($=139$) and *DP*2 ($=2828$). Note that the Ceará coastal dunes, in relation to the current average wind power (Table 1), can be either active or fixed. The model is operative for areas where precipitation, $P > 100$ mm (after Yizhaq et al. (2007)).
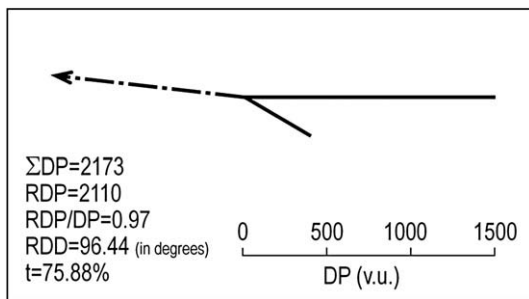
Figure 4. Sand rose of Aranaú (for 2003) on the coast of western Ceará, showing that most of the winds come from east. The value of *DP* is the yearly total wind power. *RDP* is the resultant *DP*. Note the unidirectional eastern wind (high value of *RDP/DP*). The dash-dotted arrow shows the downwind direction of the *RDP* (*RDD* in degrees). *t* is the time (in percent) during the year the wind was above the threshold of sand transport.

DP that takes on more convenient values. A *DP* is calculated separately for each wind direction that is above the threshold velocity (U_t) and is given a value known as a vector unit (v.u.). The vector units of all wind directions can be represented as a sand rose (Fig. 4). *DP* is a parameter describing the potential maximum amount of sand that could be eroded by all wind directions over the year. Hence, *DP* is a measure of the potential wind power in a sandy area.

The various vector units can be resolved into a single resultant, known as the resultant drift potential (*RDP*). The index of the directional variability of the wind is the ratio of the resultant drift potential to the drift potential (*RDP/DP*). *RDP/DP* values close to one indicate a narrow unidirectional drift potential, and values close to zero indicate a wide multidirectional drift potential. All sand roses along the Ceará coasts indicate the unidirectional easterly winds, with values of *RDP/DP* close to 1 (Fig. 4; Table 1).

The hysteresis model of Yizhaq et al. (2007) exhibits bistability with respect to wind power. The Negev Desert, area with low wind power, is covered by vegetation when rainfall is above 100 mm and wind power is low (Tsoar 2008; Fig. 3). Once dunes are covered by vegetation, an increase in wind power cannot mobilize the stable dunes because the vegetation provides an effective buffer preventing sand erosion. However under extremely high wind power this plant protection can break down (Fig. 3). If active uncovered sand dunes are accumulating under high wind power, sprouts —despite adequate rainfall — cannot thrive because of the high rate of wind erosion. The hysteretic behavior described by the model indicates that the system responds differently to increasing or decreasing values of the wind power (Tsoar, 2005).

Climatic factors and the mobility and stability of sand dunes along the Ceará coast

The coastal zone of Ceará stretches between the latitudes of 2°47'S and 4°50'S in a tropical climate. The average annual rainfall of Fortaleza between 1849 and 1999 is 1443 mm, with 88% of the rain falling during the wet season between January to June (WMSSC data obtained from http://jisao.washington.edu/data/brazil/fortaleza). There is a great inter-annual variability in precipitation over NE Brazil, with a standard deviation of 485 mm. The minimal value during this period was in 1877 (468 mm) and the maximal was in 1974 (2512 mm). The driest year in the 20th century (504 mm) was in 1958. The coastal zone is significantly wetter than the semi-arid hinterland (Auler and Smart, 2001). The average rainfall for Quixeramobim (747 mm), which is 170 km from the shoreline and SSW of Fortaleza, is 52% of that of Fortaleza (WMSSC data obtained from http://jisao.washington.edu/data_sets/wmssc/lt_mean_total_precip). These climatic conditions are caused by the widely studied Atlantic Ocean circulation pattern known as the Intertropical Convergence

Zone or ITCZ. The subtropical high pressure of the northern and southern hemispheres determines the ITCZ. This area of enhanced upward convection encircles the globe where the Northern and Southern Hemisphere tropical trade-winds collide.

Ceará's two seasons, the dry and wet ones, are determined by the position of the ITCZ. During March and April, the ITCZ is in its extreme southerly position over Ceará and the rainy period is at its peak. Precipitation then starts to decrease as the ITCZ shifts northwards, reaching its northernmost position during September and October, bringing on the dry season. If the ITCZ does not shift far enough to the south during the wet period, because of the location of the subtropical high pressure cell, there will be less rain in NE Brazil during the wet season and conditions of drought (Hastenrath, 2006).

A preliminary wind map of the Brazilian Center of Wind Energy (CBEE) indicates the existence of a narrow belt of wind with high average velocities (>8.5 m/s) along the coasts of NE Brazil from Rio Grande do Norte to the estuary of the Amazonas. This speed was found to decrease as the winds move inland (Filgueiras and Silva, 2003). The Weibull probability distribution functions were shown to provide the best fit to observed wind speed distributions (Lun and Lam, 2000). For NE Brazil, the Weibull dimensionless shape parameter (k) is very high (>3), indicative of low turbulence and low directional variability (Filgueiras and Silva, 2003).

Using Eq. 1, calculations of wind power (*DP*) for three sites located west of Fortaleza (Table 1), demonstrate that the *DP* exceeds the threshold for sand transport for more than 58% of the length of the year, most of which takes place during the dry season. The index of the wind direction variability (*RDP/DP*) is very high (0.95–0.99) along the Ceará coast, which indicates a unidirectional wind regime (namely, the easterly trade winds), which is typical for the formation of parabolic and barchan dunes. *DP* at the coasts of Ceará is also very high (compare with data in Fryberger (1979)).

The winds in Pecém (Table 1), located on the mid-Ceará coast, are easterly to south-easterly (Atlantic trade winds), which produce average drift potential (*DP*) of 692 v.u. for the years 1995–1999. Since this value of *DP* is above 400 v.u., Pecém is in a high-energy wind environment (Fryberger, 1979). *DP* data for Aranaú and Acaraú (for 2003), which are farther west, are much higher, 2173 v.u. and 1573 v.u., respectively. Wind power along the Ceará coast varies greatly from month to month and from year to year, as does precipitation, but they operate in opposite directions (Figs. 5 and 6). The monthly change in *DP* over the year shows clearly that during the wet season (January to June) *DP* is low (amounting to only 14% of the yearly *DP*), while during the dry season (July to December) it is high (86% of the yearly *DP*; Fig. 5).

Relationships among Trade-Wind Power (TWP), Sea Surface Temperature (SST) and rainfall in Ceará

As described above (Fig. 5), there is a yearly trend in wind power along the Ceará coast, an increase during the dry season and followed by a decrease in the wet season. This tendency also exists on a multiannual basis, with low precipitation (drought) years having a higher average wind speed than high precipitation years. For the period between 1948 and 1999, there is a significant ($r^2 = 0.5158$; $p < 0.001$) negative correlation in Fortaleza between annual precipitation and average wind speed at longitude 32.5°W and latitude 2.5°S (Fig. 6A).

Table 1
Wind power data from 3 coastal stations in Ceará

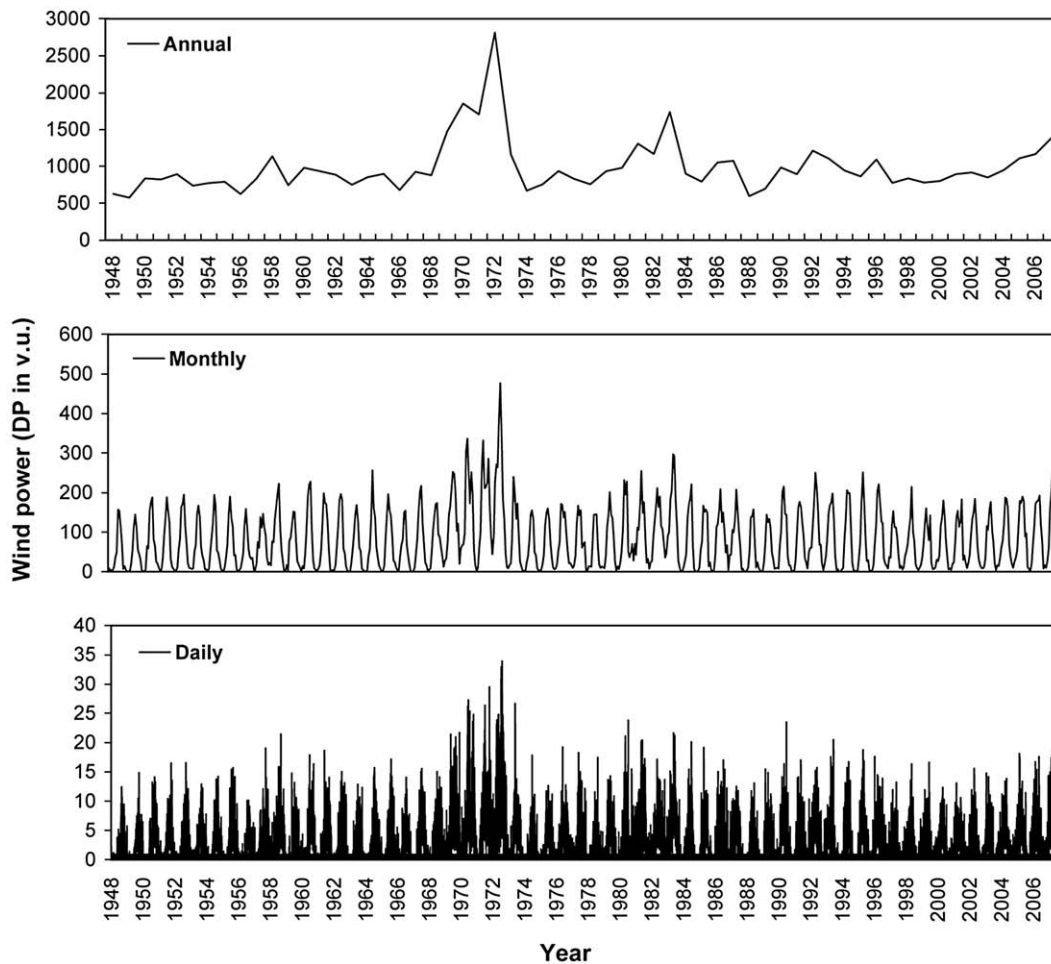| Location	DP	RDP	RDP/DP	RDD	t(%)	Year data
Pecém	692	659	0.95	99.19	58.96	1995–1999
Aranaú	2173	2110	0.97	96.38	75.88	2003
Acaraú	1573	1550	0.99	88.46	60.71	2003

See text for details.

Figure 5. The wind power (*DP*) for 60 yr (1948–2007) calculated from data of NCEP/NCAR Reanalysis at 40°W and 2.5°S with a resolution of 2.5°. Note the fluctuations in the wind power from year to year and during the year. During the wet season DP is very low and increases towards the dry season.

The average monthly rainfall in Fortaleza for 19 yr (1972–1990) correlates negatively with the TWP (*DP*) over the same period. Figure 6B shows that a power correlation gives a best fit with $r^2 = 0.91$ ($p < 0.001$). The data for Figure 6B was taken from the weather station of Fortaleza International Airport, which is 11 km west of the coastline. During the wet season, the wind power is very low, but it increases exponentially towards the dry season.

Figure 6C shows the same correlation ($p < 0.001$) for 204 months of data (1991–2007) from different coastal points, taken from the NCEP/NCAR Reanalysis. The TWP data is from 40°W and 2.5°S (model resolution of 2.5°). The rain data is from 39.4°W; 2.9°S (with model resolution of 2°). The results given in Figure 6C are similar to those of Figure 6B, where the TWP (*DP*) increases exponentially during the dry months and decreases slowly during the wet months. The scatter of the data is much higher when the rain is low (<150 mm), which indicates that during the wet season, when the monthly rainfall is high (>250 mm), the monthly *DP* is always very small.

The differences in *DP* values between the two sites (Figs. 6B and C) results from the relatively low wind power measured at Fortaleza Airport (Fig. 6B), which is far from the coastline and surrounded by city buildings, as compared with the data of Figure 6C, taken from the beach and the ocean. The differences between the trendlines of Figure 6A (linear relationship) and Figures 6B and C (power relationship) results from the definitions of wind speed and *DP*. Since wind power (*DP*) depends on the cube of the wind speed (Eq. 1), which gives much higher increases of DP for each unit increase in wind speed. The relative increase of wind power in dry years is associated with the

enhanced movement of dunes in Ceará, which depends on the intensity of the dry season (Maia et al., 2005).

More than 30 yr ago, Hastenrath and Heller (1977) and Markham and McLain (1977) showed a possible relationship between sea surface temperature (SST) anomalies over the tropical Atlantic and rainfall over NE Brazil. Drought years correspond to warm SST in the tropical North Atlantic and colder SST south of the equator, which are caused by a northward displacement of both subtropical Atlantic high pressure systems. A similar correlation exists between cold SST in the tropical South Atlantic, warm anomalies in the tropical North Atlantic and abnormally dry years in Ceará, as shown by Chung (1982). Enhanced temperature increase in the tropical North Atlantic is accompanied by a steeper meridional pressure gradient and accelerated TWP south of the equator leading to drought in northeast Brazil. This phenomenon goes hand in hand with a weakening of the TWP north of the Equator (Chiang and Koutavas, 2004; Hastenrath, 2006). This north–south SST gradient bridging the two hemispheres near the Equator is associated with a hindering of the southward migration of the ITCZ.

Average monthly figures for the southern TWP, precipitation and the differences in SST between the tropical North Atlantic and tropical South Atlantic (SST(N–S)) for a period of 17 yr (1991–2007) is presented in Figure 7. There is a significant positive correlation ($p < 0.001$) between the monthly *DP* and its corresponding SST(N–S) and significant negative correlations ($p < 0.001$) between precipitation and its corresponding *DP* and SST(N–S).

Another phenomenon influencing the region's climate is the El Niño Southern Oscillation (ENSO) cycle. Observations show that
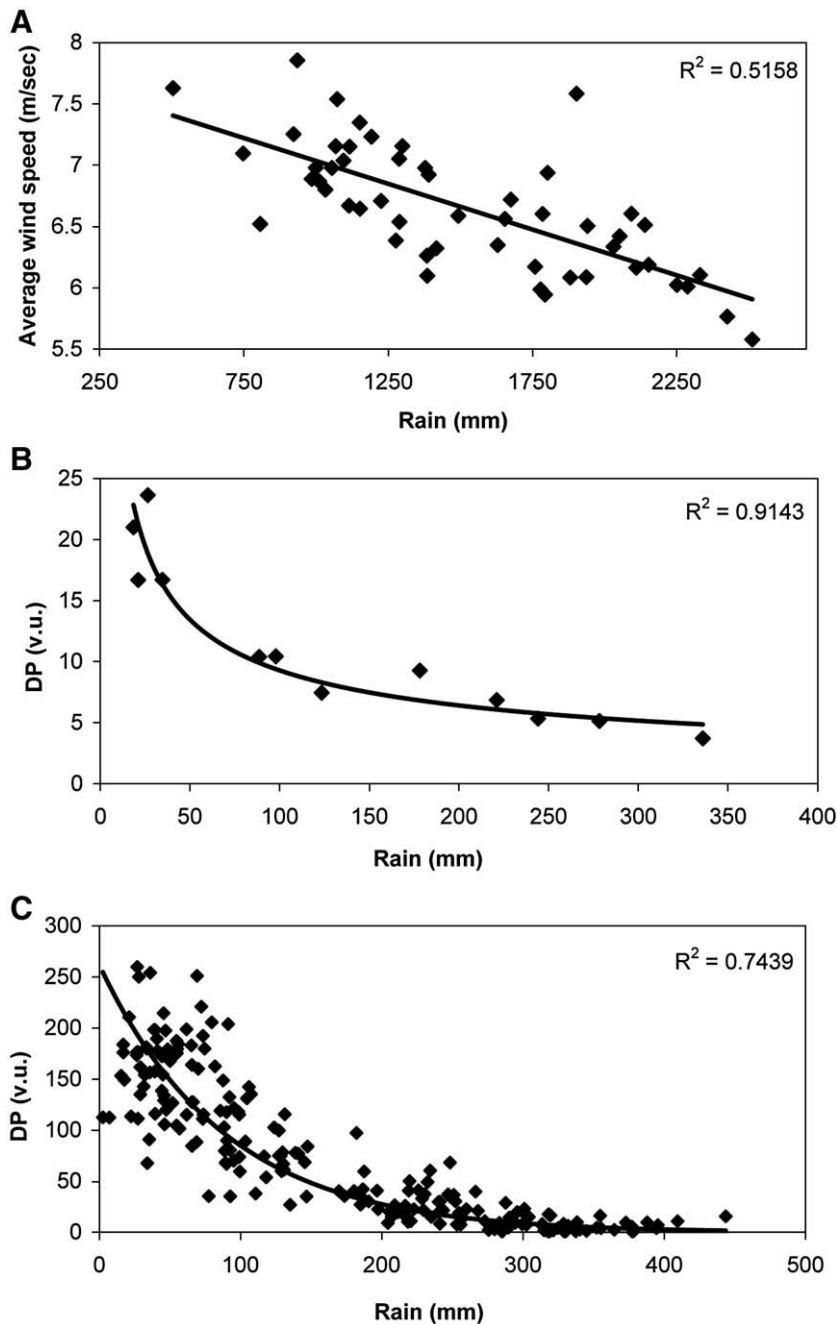
Figure 6. The correlations between average wind speed or wind power (*DP*) and rainfall. (A) Correlation on a yearly basis between average wind speed (at 32.5°W; 2.5°S) and rainfall (in Fortaleza) for 1948–1999. (B) Correlation on an average monthly basis (for 1972–1990) between DP and rainfall at Fortaleza International Airport. (C) Correlation on monthly basis between DP (from 40°W and 2.5°S) and rainfall (from 39.4°W; 2.9°S). Data from of NCEP/NCAR Reanalysis for 1991–2007.

anomalous ENSO events in the Pacific have a teleconnection with SST anomalies over the northern tropical Atlantic (Nobre and Shukla, 1996). Maia et al. (2005) found that there is a teleconnection between strong ENSO anomalies and droughts in Ceará, with marginal significance. ENSO events have not only led to increased drought periods but in some cases to increased periods of rain (Hastenrath, 2006). Hence, any relationship of ENSO to drought is dubious and, at best, has a low statistical level of significance (Gasques and Magalhes, 1987; Magalhes et al., 1988).

In conclusion, the relatively low SST in the tropical South Atlantic, which occurred when the ITCZ is shifted northwards, is associated with strong TWP over this oceanic region (Nobre and Shukla, 1996; Wang et al., 2004). The southward shift of the ITCZ weakens the northeastern trade winds over NE Brazil (Chiang et al., 2003; Hastenrath, 2006; Wang et al., 2004). These fluctuations are reflected in the present yearly shift of the ITCZ, when during the wet season, the TWP is low and the tropical South Atlantic is warmer than tropical Atlantic north of the equator. In the dry season, these parameters are reversed (Fig. 7).

Methods of field work

Sand samples were collected from stabilized sand dunes along the coast of Ceará, from Canoa Quebrada in the east to Canaà in the west (Fig. 1; Table 2). These sand samples (25 in total) were collected for luminescence dating (Aitken, 1998) and for determining the redness
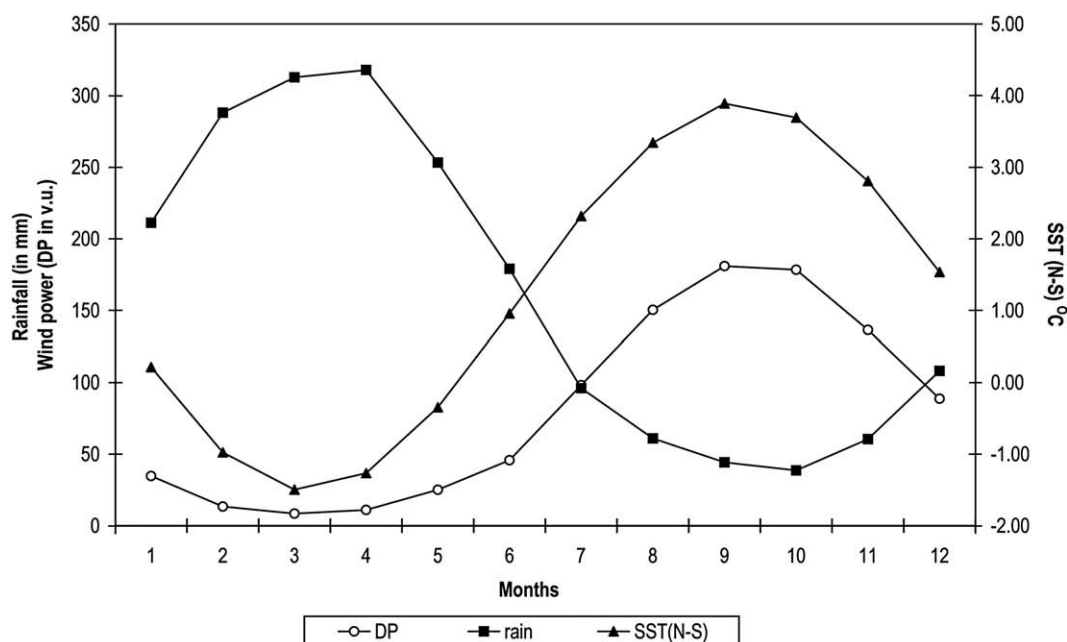
Figure 7. The relationship between the average monthly wind power (*DP*), rainfall and the differences in SST (SST(N–S) °C) between the North Atlantic (30°–60°W; 5°–20°N) and the South Atlantic (10°–30°W; 0°–20°S). The data are monthly averages for the years 1991–2007. The data were taken from the NCEP/NCAR Reanalysis. The location of the wind power data is 40°W and 2.5°S and the resolution is 2.5°. The rain data is from 39.4°W; 2.9°S, and the model resolution is about 2°.

index (RI). They were taken either by drilling to depths of >3 m with a hand auger or by a 8×20 cm PVC tube that was inserted horizontally into the walls of sand quarries or road cuts (Table 2). The luminescence-dating samples were put in or covered by black plastic bags and they were analyzed at the Dating Laboratory of the College of Technology of São Paulo and the Luminescence Dating Laboratory of the Geological Survey of Israel in Jerusalem.

Optically stimulated luminescence (OSL) was used in this study to date the dune sand samples (Table 3). The 75–180 μm quartz fractions were extracted by sieving, dissolving carbonates with HCl, oxidizing organic matter with hydrogen peroxide and etching with HF. The D_e values were measured using the single-aliquot regenerative-dose protocol (SAR; Murray and Wintle, 2000). The average D_e values and their associated errors were calculated using the central age model (Galbraith et al., 1999). Dose rates were obtained from the concentrations of *U*, Th and *K* determined by gamma spectroscopy, and the cosmic dose was calculated from the geographic location and burial depth (Table 3). For some samples, *K* was below the detection limit, and a value of 0.01% was used as the lower limit. Water contents were estimated at 3±2%. Only 12 of the 25 field-collected samples gave reliable age results (Table 3).

The color of the sand samples was determined by spectral reflectance as measured with an ASD Fieldspec spectroradiometer that covers the VIS–NIR–SWIR spectral region (0.4–2.5 μm) using a

Table 2
The location of all sand sampled from the stabilized dunes along the coast of Ceará and their redness index

Field sample number	Location	Comments	Redness Index (RI)
CE-1	Canoa Quebrada	Drilling depth 3.8 m, white sand	27
CE-2	Barra Nova	Drilling depth 3.1 m, white sand	25
CE-3	Caponga	Drilling depth 3.6 m, white sand	37
CE-4	Iguape	Drilling depth 3.25 m, red sand	1034
CE-5	Prainha	Drilling depth 3.5 m, white sand	44
CE-6	Porto do Dunas	Drilling depth 3.25 m, yellow sand	76
CE-7	Canaã	Sample from road cut, depth 2 m, reddish sand	409
CE-8	Canaã	Sample from sand quarry, white sand	59
CE-9	Canaã	Sample from road cut, yellow sand	304
CE-10	Trairi	Sample from road cut, red sand	737
CE-11	Trairi	Sample from sand quarry, red sand	862
CE-12	Lagoinha	Close to the beach, discernable dune structure, dark minerals, reddish sand	194
CE-13	Lagoinha	Sample from sand quarry, reddish sand	147
CE-14	Lagoinha	Sample from sand quarry, red sand	653
CE-15	Lagoinha	Sample from sand quarry, red sand	936
CE-16	Taiba	From dune's plinth, yellow sand	86
CE-17	Taiba	Sample from road cut, discernable dune structure, yellow sand	79
CE-18	Colonia	Sample 1 m from dune's crest, discernable dune structure, white sand w/dark minerals	32
CE-19	Pecém	Sample from road cut, yellow sand	192
CE-20	Pecém	Sample from road cut, red sand	452
CE-21	Pecém	Sample from road cut, red sand	358
CE-22	Pecém	Sample from sand quarry, reddish sand	107
CE-23	Coité–Pecém	Sample from sand quarry, white sand	16
CE-24	Coité–Pecém	Sample from sand quarry, red sand	786
CE-25	Coité–Pecém	Sample from sand quarry, white sand	8

Table 3
Luminescence dating results

Laboratory sample number	Field sample number	Location	Comments	Depth (m)	SAR De (Gy)	Over-dispersion (%)	Cosmic Dose (μGy/a)	Beta Dose (μGy/a)	Gamma Dose (μGy/a)	Total dose (μGy/a)	SAR Age (ka)
1731	CE-2	Barra Nova	Drilling	3.1	0.13±0.03	0	111	181	227	523±21	**0.25±0.05**
1733	CE-4	Iguape	Drilling	3.25	73±5	23	107	200	242	553±27	**132±11**
1735	CE-6	Porto do Dunas	Drilling	3.25	1.9±0.2	26	107	609	386	1107±65	**1.75±0.2**
1741	CE-12	Lagoinha	Heavy minerals	2	0.25±0.05	51	142	1617	1309	3085±138	**0.08±0.02**
1742	CE-13	Lagoinha	Sand quarry, red sand	2	81±8	24	142	1109	731	1992±111	**40.8±4.6**
1743	CE-14	Lagoinha	Red sand	1.5	11.8±1.0	19	156	387	413	963±33	**12.3±1.2**
1744	CE-15	Lagoinha	Red sand	1	55±4	16	170	1287	918	2387±128	**22.9±2.0**
1748	CE-19	Pecém	Road cut, white sand	1	8.9±0.5	21	170	841	521	1537±94	**5.8±0.5**
1750	CE-21	Pecém	Road cut, red sand	2	7.5±0.3	15	142	549	427	1125±47	**6.7±0.4**
1751	CE-22	Pecém	Sand quarry, red sand	3	22.4±0.8	8	114	1159	691	1973±126	**11.4±0.8**
1753	CE-24	Coité–Pecém	Sand quarry, red sand	3	24.9±2.8	26	114	289	256	663±34	**37.6±4.7**
1754	CE-25	Coité–Pecém	Sand quarry, white sand	4	69±3	19	86	1206	529	1823±169	**37.7±3.9**

Field sample number is the same as for Table 2. De was measured using the optically stimulated luminescence signal and the single aliquot regenerative dose protocol. All samples showed good preheat plateaus, but some of the samples had poor recycling ratios and a substantial IR signal. Errors on the De were calculated using the Central Age Model (Galbraith et al., 1999). Over dispersion is the scatter in the measurements that are beyond the normal distribution. Total dose includes an alpha contribution of 3–18 μGy/a (not shown in Table).

self-illuminating contact probe. Twenty spectral reflectance measurements were taken for each sample and averaged to present the spectral characteristics of each sample. This was repeated for each sample from four directions, and the resulting spectra were then averaged, to avoid biases related with Bidirectional Reflectance Distribution Function. The free iron-oxide content of the sand was estimated by the Redness Index (RI), which is significantly correlated with free iron oxide content (Ben-Dor et al., 2006; Tsoar et al., 2008). The redness index (RI) is determined from the spectral reflectance ratio given in Eq. 2 (Mathieu et al., 1998):

$$RI = \frac{R^2}{B * G^3} \qquad (2)$$

where R is the reflectance in the visible red (640 nm), G, in the visible green (510 nm) and B, in the visible blue (460 nm) wave bands.

Results

The luminescence ages of the 12 samples range from 132 ka to sub-recent (Table 3) and show that stabilization of the coastal dunes of Ceará has existed since the end of the penultimate glacial period. Many of the dunes were stabilized during the last glacial period, however the errors on the ages are mostly greater than 10%, precluding the correlation of these ages with specific short climatic events.

The oldest age of 132±11 ka falls at the end of the glacial period known as the marine oxygen-isotope stage 6 (OIS6), but the large error can also place it at the beginning of the interglacial OIS5. Three samples were dated to between 38 ka and 41 ka (37.6±4.7 ka, 37.7±3.9 ka and 40.8±4.6 ka), and may be correlated to Heinrich event 4 which falls at ~37–38 ka. One sample falls on the LGM or H2 (22.9±2.0 ka). Two samples are from the early Holocene (12.3±1.2 ka and 11.4±0.8 ka) and they could be correlated with the Younger Dryas at 12.7–11.5 ka. Two samples have recent ages (80 and 250 yr), which may result from recent remobilization of stable dunes or artificial stabilization of active dunes. Two samples give ages of the middle Holocene (5.8±0.5 ka and 6.7±0.4 ka), one of them may indicate a period of glacial advance (Ellwood et al., 1997).

The coastal dune sand has different hues from very white (CE-25) to red sand (sample CE-4). The redness comes from iron oxide mine-

rals coating the quartz grains (Pye and Tsoar, 1990; Wopfner and Twidale, 1988). It is accepted that beach sand is very white, but it reddens with time via oxidation, which persists as long as the sand is exposed to air (Ben-Dor et al., 2006; Norris, 1969). Hence, the redness rate or the percentage of iron oxide in sand dunes grains may indicate their age (Folk, 1976; Gardner and Pye, 1981; Norris, 1969; Walker, 1979; White et al., 1997; Wopfner and Twidale, 1988). The sample with the highest value of RI (= 1034) is also the oldest samples (CE-4, which is 132±11 kyr). However, there is no significant correlation between the luminescence ages and the RI. The results (Table 2) are similar to those of Levin et al. (2007) on the sand dunes of Lençóis Maranhenses, further to the west, where the effect of inter-dune freshwater pools on the bleaching of the red color of dune sand was inferred.

Discussions

There is a negative correlation between the two paleoclimatological parameters, rainfall and wind power (DP). It is based on observations of wind power changes over a long period that includes many dry and wet years (Fig. 6A), as well as annual changes during the wet season and dry season (Figs. 6B and C), demonstrating the negative connection between rainfall and DP (Fig. 7). The extent of seasonal southward shift of the ITCZ, which currently determines the wet or dry years along the coast of Ceará State, could last for decades or centuries during the Late Quaternary. This frequent change of climatic temperatures and the consequent shift in the ITCZ can be a result of rapid changes between interstadial and stadial times (Peterson et al., 2000). During these stadial periods, the average rainfall over the coasts of Ceará State was higher than at present and, in particular, the wind power was much lower. During warmer periods of the Late Pleistocene, when the ITCZ migrated north of its present average location, the coasts of Ceará had less rain but mainly much higher wind power.

Determinations of dry and wet years in NE Brazil, with the aid of speleothems and travertine deposits, clearly delineate fluctuations in climate (Wang et al., 2004). Terrigenous sediments found in core material from the upper continental slope of NE Brazil, indicate much wetter past climates (Arz et al., 1998; Auler and Smart, 2001; Rahmstorf, 2003). These wet periods correlate with cold periods known as Heinrich events as well as with the Dansgaard–Oeschger

(DO) heating and cooling cycles known from short-term climatic variations recorded in Greenland ice cores, which influence the intensity of the South Atlantic trade-winds (Bond and Lotti, 1995; Little et al., 1997; Arz et al., 1998).

Wang et al. (2004) suggest that the pluvial periods occurred when the southerly limit of the ITCZ was several hundred km south of its present limit. They found that speleothem samples grew rapidly during relatively short intervals (several hundreds of years) within glacial periods of the last 210 kyr. According to the GISP2 climate record of the last glaciation, there were about 20 DO events, each of which was characterized an abrupt change of climate going from a relatively warm period to a cold one. These events occur on a regular cycle of 1470 yr, but have irregular amplitude (Genty et al., 2003; Rahmstorf, 2003). Abrupt climate changes were not confined to the last glaciation, but also appear during the former interglacial period (Dansgaard et al., 1993).

These pluvial intervals in Ceará correspond to the periods of light color reflectance of Cariaco Basin sediments north of Venezuela (Peterson et al., 2000). These changes were inferred to result from a southward shift of the northernmost position of the ITCZ, which decreased rainfall in this northern part of South America.

As mentioned above, there were many cycles of abrupt warm-to-cool climatic changes during the last glacial period. The shortest cycle is of 1470 yr, but such short cycles cannot be correlated with on the basis of the presented luminescence ages. The luminescence age of a dune determines the approximate time of the start of dune stabilization, which correspond to periods with deep southern shift of the ITCZ, and the resultant decrease in speed of the trade winds. Because of the high resolution of the $\delta^{18}O$ of GISP2 ice core determinations and the low resolution of the luminescence ages, it is not always possible to attribute the dune stabilization time to a specific colder period in the core record (Chiang et al., 2003; Rahmstorf, 2003).

We infer that dune activity in Ceará during the dry years resulted from higher wind power, and not low precipitation. During 151 yr of record (1849–1999), which are considered in general as a semi-arid period, known for the occurrence of anomalous, strong droughts (Hastenrath and Heller, 1977; Hastenrath, 2006), the minimal rainfall in Fortaleza was 468 mm. This level of precipitation, which soaks easily into sand, provides sufficient soil moisture to support the dune's vegetation cover (Tsoar, 2008; Tsoar et al., 2008). Hence, the lack of vegetation on sand dunes during a dry period (as it is today) is due to high wind power (Fig. 7) and not to the low level of rain. In periods when wind power was much lower and rainfall higher, vegetation could develop on some of the dunes. However, it was the low wind power that initiated the vegetation cover (and stabilization) and not the increase in rainfall, which does not add supplementary moisture to the dune sand but rather to the ground water (Tsoar, 2004).

The whitening of old sand in the stabilized dunes is typical for tropical coasts. The accumulation of highly dynamic sand dunes along a coast blocks the outlet of runoffs, leading to the formation of freshwater lagoons in front of the dunes. The high amount of rainfall over the dunes also causes an increase in water table levels over the rainy season. In the anaerobic conditions that develop, microorganisms reduce the reddish trivalent Fe oxide to a colorless bivalent Fe hydroxide (Levin et al., 2007). All the white sand dunes sampled were affected by freshwater lagoons or a high water table. Two samples, CE-24 and CE-25 were taken from the same sand quarry, where the red sand (CE-24) overlies the white sand (CE-25). These two samples are of the same age of ~38 ka (Table 3) and have identical grain-size distributions. We infer that the CE-24 and CE-25 samples were part of the same stabilized dune. Seemingly, the ground water table under which reduction of the trivalent Fe took place had a level that reached to the line that now differentiates the upper red layer from the lower white one.

Conclusions

The vast prevalence of active sand dunes along the coast of NE Brazil in a tropical climate (average yearly rainfall above 1000 mm) results from the high powered trade winds, mostly during the dry season. Many stabilized dunes are found along this coast, side by side with the active dunes. A hysteresis model based on changes in wind power can explain the co-existence of stabilized and active dunes in the same area.

Vegetation on sand dunes in NE Brazil thrives when the rainfall is above 400 mm and the wind power is low. There are many indications of wetter periods in NE Brazil during the Late Quaternary. The wind power during wet periods before the instrumental record may have been much lower than at present, based on the instrumental record and the location of the ITCZ. The dunes during the wetter periods were stabilized by vegetation due to low wind power and not because of the increased precipitation.

Luminescence dating of the sand of the some of the stabilized dunes shows that the dunes along the coasts of Ceará State were stabilized during various periods over the last 130 ka. Most of these may be associated with colder events in the northern Hemisphere, characterized by glaciation, such as the Heinrich events or Younger Dryas. Since most of the stabilized dunes that were sampled for luminescence dating were stabilized for a very long period, it is assumed that all the droughts during the last 130 ka did not cause mobility of the stabilized sand dunes in NE Brazil.

Some of these old stabilized dunes are composed of red sand, while others are much whiter. There is no correlation between sand redness and the time of stabilization. We assume that reduction of the trivalent Fe to bivalent Fe was performed by organisms growing in high water tables in contact with the dunes or in lagoons formed during high precipitation periods, when river drainage into the Atlantic Ocean was blocked by the encroaching dunes.

Acknowledgments

References

Aitken, M.J., 1998. An Introduction to Optical Dating. Oxford University Press, Oxford.

Arz, H.W., Patzold, J., Wefer, G., 1998. Correlated millennial-scale changes in surface hydrography and terrigenous sediment yield inferred from last-glacial marine deposits of northeastern Brazil. Quaternary Research 50, 157–166.

Ash, J.E., Wasson, R.J., 1983. Vegetation and sand mobility in the Australian desert dunefield. Zeitschrift fur Geomorphologie N.F., Supplementbande 45, 7–25.

Auler, A.S., Smart, P.L., 2001. Late quaternary paleoclimate in semiarid northeastern Brazil from U-Series dating of travertine and water-table speleothems. Quaternary Research 55, 159–167.

Ben-Dor, E., Levin, N., Singer, A., Karnieli, A., Braun, O., Kidron, G.J., 2006. Quantitative mapping of the soil rubification process on sand dunes using an airborne hyperspectral sensor. Geoderma 131, 1–21.

Bond, G.C., Lotti, R., 1995. Iceberg discharges into the North-Atlantic on millennial time scales during the last glaciation. Science 267, 1005–1010.

Castro, J.W.A., 2005. Burying processes carried out by a mobile transversal dunefield, Paracuru County, State of Ceara, Brazil. Environmental Geology 49, 214–218.

Chiang, J.C.H., Koutavas, A., 2004. Climate change — tropical flip-flop connections. Nature 432, 684–685.

Chiang, J.C.H., Biasutti, M., Battisti, D.S., 2003. Sensitivity of the Atlantic intertropical convergence zone to last glacial maximum boundary conditions. Paleoceanography 18.

Chung, J.C., 1982. Correlations between the tropical Atlantic trade winds and precipitation in northeastern Brazil. International Journal of Climatology 2, 35–46.

Claudino-Sales, V., Peulvast, J.P., 2002. Dunes generation and ponds on the coast of Ceara State (Northeast Brazil). In: Allison, R.J. (Ed.), Applied Geomorphology. John Wiley & Sons, Chichester, pp. 443–460.

Dansgaard, W., Johnsen, S.J., Clausen, H.B., Dahljensen, D., Gundestrup, N.S., Hammer,

C.U., Hvidberg, C.S., Steffensen, J.P., Sveinbjornsdottir, A.E., Jouzel, J., Bond, G., 1993. Evidence for general instability of past climate from a 250-kyr ice-core record. Nature 364, 218–220.

De Oliveira, P.E., Barreto, A.M.F., Suguio, K., 1999. Late Pleistocene/Holocene climatic and vegetational history of the Brazilian caatinga: the fossil dunes of the middle Sao Francisco River. Palaeogeography Palaeoclimatology Palaeoecology 152, 319–337.

Ellwood, B.B., Petruso, K.M., Harrold, F.B., 1997. High-resolution paleoclimatic trends for the Holocene identified using magnetic susceptibility data from archaeological excavations in caves. Journal of Archaeological Science 24, 569–573.

Filgueiras, A., Silva, T., 2003. Wind energy in Brazil — present and future. Renewable & Sustainable Energy Reviews 7, 439–451.

Folk, R.L., 1976. Reddening of desert sands: Simpson desert, Northern Territory, Australia. Journal of Sedimentary Petrology 46, 604–615.

Fryberger, S.G., 1979. Dune forms and wind regime. In: McKee, E.D. (Ed.), Geological Survey Professional Paper, 1052. U.S. Geological Survey, Washington. U.S., pp. 137–169.

Galbraith, R.F., Roberts, R.G., Laslett, G.M., Yoshida, H., Olley, J.M., 1999. Optical dating of single and multiple grains of quartz from Jinmium rock shelter, northern Australia: Part I. Experimental design and statistical models. Archaeometry 41, 339–364.

Gardner, R., Pye, K., 1981. Nature, origin and palaeoenvironmental significance of red coastal and desert dune sands. Progress in Physical Geography 5, 514–534.

Gasques, J.G., Magalhes, A.R., 1987. Climatic anomalies and their impact in Brazil during the 1982–83 ENSO event. In: Glantz, M., Katz, R., Krenz, M. (Eds.), The Societal Impacts Asociated with the 1982–83 Worldwide Climate Anomalies. National Center for Atmospheric Research, Boulder, pp. 30–36.

Genty, D., Blamart, D., Ouahdi, R., Gilmour, M., Baker, A., Jouzel, J., Van-Exter, S., 2003. Precise dating of Dansgaard–Oeschger climate oscillations in western Europe from stalagmite data. Nature 421, 833–837.

Hastenrath, S., 2006. Circulation and teleconnection mechanisms of Northeast Brazil droughts. Progress in Oceanography 70, 407–415.

Hastenrath, S., Heller, L., 1977. Dynamics of climatic hazards in Northeast Brazil. Quarterly Journal of the Royal Meteorological Society 103, 77–92.

Jimenez, J.A., Maia, L.P., Serra, J., Morais, J., 1999. Aeolian dune migration along the Ceara coast, north-eastern Brazil. Sedimentology 46, 689–701.

Lancaster, N., 1988. Development of linear dunes in the southwestern Kalahari, Southern Africa. Journal of Arid Environments 14, 233–244.

Levin, N., Tsoar, H., Maia, L.P., Sales, V.C., Herrmann, H., 2007. Dune whitening and inter-dune freshwater ponds in NE Brazil. Catena 70, 1–15.

Little, M.G., Schneider, R.R., Kroon, D., Price, B., Summerhayes, C.P., Segl, M., 1997. Trade wind forcing of upwelling, seasonality, and Heinrich events as a response to sub-Milankovitch climate variability. Paleoceanography 12, 568–576.

Lun, I.Y.F., Lam, J.C., 2000. A study of Weibull parameters using long-term wind observations. Renewable Energy 20, 145–153.

Magalhes, A.R., Filho, H.C., Garagorry, F.L., Gasques, J.G., Molion, L.C.B., Neto, M., de, S.A., Nobre, C.A., Porto, E.R., Reboucas, O.E., 1988. The effects of climatic variations on agriculture in Northeast Brazil. In: Parry, M.L., Carter, T.R., Konijn, N.T. (Eds.), The Impacts of Climatic Variations on Agriculture. Kluwer Academic Publications, Dordrecht, pp. 273–380.

Maia, L.P., Freire, G.S.S., Lacerda, L.D., 2005. Accelerated dune migration and aeolian transport during El Nino events along the NE Brazilian coast. Journal of Coastal Research 21, 1121–1126.

Markham, C.G., McLain, D.R., 1977. Sea-surface temperature related to rain in Ceara, Northeastern Brazil. Nature 265, 320–323.

Mathieu, R., Pouget, M., Cervelle, B., Escadafal, R., 1998. Relationships between satellite-based radiometric indices simulated using laboratory reflectance data and typic soil color of an arid environment. Remote Sensing of Environment 66, 17–28.

Middleton, N., Thomas, D.S.G., 1997. World Atlas of Desertification. UNEP/Edward Arnold, London.

Murray, A.S., Wintle, A.G., 2000. Luminescence dating of quartz using an improved single-aliquot regenerative-dose protocol. Radiation Measurements 32, 57–73.

Nobre, P., Shukla, J., 1996. Variations of sea surface temperature, wind stress, and rainfall over the tropical Atlantic and South America. Journal of Climate 9, 2464–2479.

Norris, R.M., 1969. Dune reddening and time. Journal of Sedimentary Petrology 39, 7–11.

Peterson, L.C., Haug, G.H., Hughen, K.A., Rohl, U., 2000. Rapid changes in the hydrologic cycle of the tropical Atlantic during the last glacial. Science 290, 1947–1951.

Pye, K., Tsoar, H., 1990. Aeolian Sand and Sand Dunes. Unwin Hyman, London.

Rahmstorf, S., 2003. Timing of abrupt climate change: a precise clock. Geophysical Research Letters 30 (NO. 10), 1510 1510.1029/2003GL017115.

Tsoar, H., 2004. Sand dunes. In: Hillel, D. (Ed.), Encyclopedia of Soils in the Environment. Elsevier, Oxford, pp. 462–471.

Tsoar, H., 2005. Sand dunes mobility and stability in relation to climate. Physica A 357, 50–56.

Tsoar, H., 2008. Land use and its effect on the mobilization and stabilization of the NW Negev sand dunes. In: Breckle, S.W., Yair, A., Veste, M. (Eds.), Arid Dune Ecosystems. Springer, Berlin, pp. 79–89.

Tsoar, H., Blumberg, D.G., Wenkart, R., 2008. Formation and geomorphology of the NW Negev sand dunes. In: Breckle, S.W., Yair, A., Veste, M. (Eds.), Arid Dune Ecosystems. Springer, Berlin, pp. 25–48.

Walker, T.R., 1979. Red color in dune sand. In: McKee, E.D. (Ed.), A Study of Global Sand Seas. Professional Paper, 1052. U.S. Geological Survey, Washington. U.S., pp. 137–169.

Wang, X.F., Auler, A.S., Edwards, R.L., Cheng, H., Cristalli, P.S., Smart, P.L., Richards, D.A., Shen, C.C., 2004. Wet periods in northeastern Brazil over the past 210 kyr linked to distant climate anomalies. Nature 432, 740–743.

Wasson, R.J., 1984. Late Quaternary palaeoenvironments in the desert dunefields of Australia. In: Vogel, J.C. (Ed.), Late Cainozoic Palaeoclimates of The Southern Hemisphere. A.A. Balkema, Rotterdam, pp. 419–432.

White, K., Walden, J., Drake, N., Eckardt, F., Settle, J., 1997. Mapping the iron oxide content of Dune sands, Namib Sand Sea, Namibia, using Landsat Thematic Mapper data. Remote Sensing of Environment 62, 30–39.

Wopfner, G., Twidale, C.R., 1988. Formation and age of desert dunes in the Lake Eyre depocentres in central Australia. Geologische Rundschau 77, 815–834.

Yizhaq, H., Ashkenazy, Y., Tsoar, H., 2007. Why do active and stabilized dunes coexist under the same climatic conditions? Physical Review Letters 98 Art. No. 188001 MAY 188004 182007.